Methods for increasing the potential of integration of EV chargers into the DC catenary of electric transport grids
A trolleygrid case study

van der Horst, Koen; Diab, Ibrahim; Chandra Mouli, Gautham Ram; Bauer, Pavol

DOI
10.1016/j.etran.2023.100271

Publication date
2023

Document Version
Final published version

Published in
eTransportation

Citation (APA)
van der Horst, K., Diab, I., Chandra Mouli, G. R., & Bauer, P. (2023). Methods for increasing the potential of integration of EV chargers into the DC catenary of electric transport grids: A trolleygrid case study. *eTransportation*, *18*, Article 100271. https://doi.org/10.1016/j.etran.2023.100271

eTransportation 18 (2023) 100271

Contents lists available at ScienceDirect

eTransportation

journal homepage: www.journals.elsevier.com/etransportation

Methods for increasing the potential of integration of EV chargers into the DC catenary of electric transport grids: A trolleygrid case study

Koen van der Horst, Ibrahim Diab *, Gautham Ram Chandra Mouli, Pavol Bauer

Technische Universiteit Delft, Mekelweg 4, Delft, 2628 CD, Zuid Holland, The Netherlands

ARTICLE INFO

Keywords:
DC grids
EV chargers
PV system
Transportation
Trolleygrids

ABSTRACT

The traction substations of urban electric transport grids are oversized and underutilized in terms of their capacity. While their over-sizing is an unfortunate waste, their under-utilization creates the major hurdle for the integration of renewables into these grids due to the lack of a base load. Therefore, integrating smart grid loads such as EV chargers is not only an opportunity but a necessity for the sustainable transport grid of the future.

This paper examines six methods for increasing the potential of EV chargers in three case studies of a trolleygrid, namely a higher substation no-load voltage, a higher substation power capacity, a smart charging method, adding a third overheard parallel line, adding a bilateral connection, and installing a multi-port converter between two substations. From the case studies, the most promising and cost-effective method seems to be introducing a bilateral connection, bringing a charging capacity for up to 175 electric cars per day. Meanwhile, other costly and complex methods, such as smart charging with grid state sensors and communication, can offer charging room for over 200 electric cars per day. Furthermore, using solar PV systems to power the grid showed a more than doubling of the directly utilized energy by installing a 150kW charger, from 19% to 41%. This reduces the power mismatch between the trolleygrid and the PV system from 81% to 59% and thereby reduces the severe economic need for storage, AC grid power exchange, or PV power curtailment while allowing a high penetration of renewables.

1. Introduction

Today, EV charging infrastructures are a critical bottleneck for the diffusion of electric vehicles (EVs). The barrier is the unavailability of spare charging capacity in the increasingly congested electricity grids that are not designed for more of such high, variable, and inconsistent power demands [1–4].

For this, urban electric public transport networks are being researched to host smart grid loads, like EV chargers, by integrating them into their infrastructures [5–10]. This is because these grids are historically sized for the worst-case scenarios of power demand, and can be better utilized by smart grid loads and appropriate power management. Indeed, many works are already rethinking these transport networks as multi-functional, active grids by integrating into them renewable energy sources (RES) [8,11], storage systems [12–15], EV chargers [9,10,16], and other smart grid loads and fleets [7,17–20].

There is also a benefit for the transport grids as this creates a base load on their substations in the moments of no vehicle traffic. This can reduce the need for expensive storage systems when, for example, a solar PV system is connected to the traction substation. This can be illustrated by the example of Fig. 1 of the trolleybus grid of Arnhem, the Netherlands, where the lack of a base load jeopardized the techno-economic feasibility of the integration of renewables [8,21].

1.1. Integration of EV chargers in public electric transportation grids

The integration of EV chargers directly into transport infrastructures is an emerging topic. While a number of studies exist on this theme, they mostly deal with simplified grid models and/or an lumped-energy methodology that does not consider the operational violations on the DC side of the transportation grid that an extra charging load could bring. Unfortunately, this is often overlooked in literature, and while some works already tackle the integration of EV chargers in transport grids such as trams and trolleybuses (Table 1), they deal mostly with:

- Simplified grid models that do not calculate and/or consider the resulting grid power, voltage, and current violations, and/or
- An analysis of measurements that offer insight only to one case of a relatively small charger, and does not quantify the potential of the grid beyond it, and/or

* Correspondence to: Electrical Sustainable Energy department, TU Delft, 2628 CD Delft, The Netherlands.
E-mail address: i.diab@tudelft.nl (I. Diab).

https://doi.org/10.1016/j.etran.2023.100271
Received 28 October 2022; Received in revised form 15 July 2023; Accepted 30 July 2023
Available online 1 August 2023

Table 1
Overview of the projects with the integration of EV chargers into traction networks powering trolleybuses and trams.

Location	Traction network	Description/objective
Solingen, Germany [17,22–25]	Trolleybus	Investigating the potential of integrating decentralized renewable power generation (e.g., photovoltaics), charging stations for EVs, and stationary battery storage into the existing DC trolleybus infrastructure.
Gdynia, Poland [16,26–29]	Trolleybus	Analyzing the available capacity of the traction grid of Gdynia to charge electric cars. Furthermore, Smart Grids solutions for urban traction supply systems are introduced to improve the efficiency and stability of the traction network.
Edinburgh, Scotland [30–32]	Tram	Electrical capacity for EV charging systems based on four different charging control strategies are assessed and tested on the public tram system. The various connection topology, earthing methods, and stability criteria are considered.
Lisbon, Portugal [33]	Tram	Integration of bidirectional EV chargers into a DC catenary grid for trams. The authors looked into the concept V4G with an associated fuzzy control method. Furthermore, the benefits of an energy storage system in a catenary grid are demonstrated.
Sheffield, UK [34,35]	Tram	Method to improve the energy efficiency of trams with the use of static energy storage systems and EV batteries in the public tram network. Current flow measurements and tram GPS data were used to simulate the energy flow in the catenary grid using a MATLAB/Simulink model.

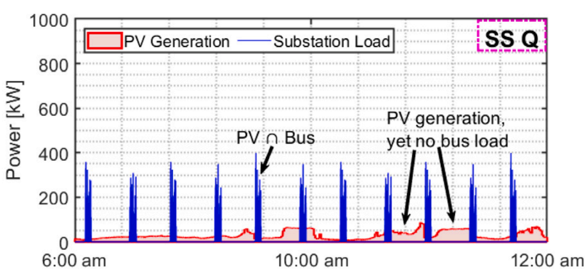

Fig. 1. Simulation results showing the mismatch between solar PV generation and substation demand in the trolleygrid of Arnhem [8].

- A focus on harvesting the baseline spare capacity of a specific EV charger case study, but without offering insights on how to increase this capacity and/or optimize the EV charger placement
- A focus on a local case study without an analysis that could serve the extrapolation of the results beyond the local studied grid

To start with the first point: As mentioned, transportation grids are oversized to account for rare occurrences of high power demands. These moments should still be considered when integrating EV chargers so as not to violate the substation power rating. However, same as with the maximum power limit, there are maximum line current and minimum line voltage limitations dictated by the overhead cable temperature limit and the vehicle current collector, respectively. Table 2 gives an example of the limitations of the trolleygrid of the city of Arnhem, the Netherlands, which is the studied case study city later in this paper. It is then important for any transport grid study to consider all three violations simultaneously. Meanwhile, none of the studied cities reported in Table 1 account for this.

For example, the work in Gdynia [16] starts with historical measurements of the minimum line voltage and adds to them an estimated voltage drop based on the superposition principle. This approach has three limitations: First, the transport grid deals with (mechanical) power-source loads whose power flow cannot be accurately computed linearly by the superposition principle. Second, the superposition principle would ignore the combined voltage drop effect of all the load currents at the substation feeder cable (additional non-linearity in the solution). Third, the moments of maximum power, current, and voltage do not necessarily occur at the same moment; hence, a historical maximum/minimum of each parameter cannot be studied independently. For example, a high load near the substation would not necessarily create a large voltage drop. This is why *instantaneous* measurements or simulations of the current, voltage, and power must be *simultaneously* studied. Beyond this work, other studies either ignore studying the voltage drop, such as the works in Edinburgh [31] or Sheffield [34], or look only at averaged values of the voltage drops and not in absolute terms such as the work in Solingen [24], or overlook the reported line voltages as low as 350 V such as the Lisbon study [33].

Regarding the second point, on the vehicle charger size, the study of Gdynia [16] and Lisbon [33] look at one fast charger up to 50 kW, while the study in Solingen [24] goes up to 132 kW in steps of 22 kW. Meanwhile, the study in Sheffield [34] only mentions the advantages of EV charging, and the study in Edinburgh [31] finds an energy equivalent of the available EV charging power from the spare energy capacity afforded from historical substation measurements.

Regarding the third point, only the Edinburgh [31] study looks at the maximal achievable EV potential from the grid, while the other studies suffice themselves with one charger. Still, unlike the work proposed in our paper here, none of the studies attempt to study methods to increase this EV potential beyond the instances of first violations of Power, Voltage, and/or Current.

Finally, all of the studies limit themselves to investigating their local case study, without any analysis that could serve as lessons-learned and extrapolation to other transport grids based on their local traffic intensity, section lengths, and desired EV charger location along the line.

1.2. *Paper contributions*

This paper offers the following contributions:

1. Three detailed case studies of EV charger integration in electrical public transport grids that use comprehensive and verified vehicle, grid, and *simultaneously* takes into account the effect on the grid power, voltage, and current violations, as opposed to the less comprehensive studies in the literature that focus only on one or two of the three violations, while using simplified grid models
2. Detailed comparison of six methods for *increasing* the EV charger integration potential, namely a higher substation voltage, a higher substation power capacity, a smart charging method, adding a third overheard parallel line, adding a bilateral connection, and installing a multi-port converter, in terms of quantifying their additional EV charging potential at any location on a general trolleygrid section
3. An analysis and thereafter a general extrapolation of the three case study results into a set of generalizable suggestions on the sizing and placement of EV chargers in any section of a given trolleygrid depending on the traffic intensity, section length, and desired EV charger location along the line

Table 2
Example of trolleygrid limitations: Arnhem, the Netherlands.

Violation	Limitation	Allowable continuous duration
Maximum Substation Power[a]	$100\% < P_s \leq 120\%$ $P_s > 120\%$	10 consecutive seconds Never
Minimum Line Voltage	$400\text{V} < V_{min} < 500\text{V}$ $V_{min} \leq 400$ V	120 s [36] Never [37]
Maximum Current	$I_{max,1} < 880$ A $I_{max,2} < 1200$ A	50 min [16,23] 30 min [38]

[a]Limit currently tolerated by the trolleygrid operator.

1.3. Paper structure

The paper starts with an introduction to EV chargers in public electric transport grid in Section 1, and suggests six methods in Section 2 for increasing this integration potential. Section 3 presents the modeling methodology for the various subsystems of the simulations used in the three case studies of this paper: The theoretical case study of Section 4, and the two case studies of Arnhem, The Netherlands, in Section 5. Section 6 offers a summary of the recommendations of this work in terms of the sizing and placement of EV chargers in electric public transport networks. Finally, Section 7 closes with recommendations and future works.

2. EV chargers in trolleygrids

2.1. The trolleybus and the trolleygrid

The trolleybus is an electric bus that is supplied by overhead lines (catenary), similar to the way a tram operates. Changing attitudes toward diesel buses is bringing trolleybuses back into the transportation landscape as a key player in transportation electrification [39]. Trolleybuses consume about 70 kW during regular driving and can reach demands higher than 300 kW while accelerating. When a trolleybus brakes, the available regenerative braking power can be as high as 200 kW. While some solutions exist, for example, with on-board storage devices, this harvestable energy, is frequently wasted in on-board braking resistors.

Fig. 2 shows the typical layout of a trolleygrid. For reasons such as faults and transmission losses, the trolleybus lines are divided into isolated sections of few hundreds of meters, up to 1 or 2 km, depending on the trolleygrid city. The power comes from the Low Voltage AC grid (LVAC) and a transformer steps down the voltage, then a rectifier converts into to DC, as the buses run at a nominal voltage of 600–700 V. The minimum voltage, due to transmission voltage drops, that the bus runs on is 400 V.

The transformer-rectifier system is housed in a “substation”. One substation can feed one or more sections, to which it is connected via the section feeder cables (FC). In Fig. 2, substation 1 feeds two sections, while substation 2 feeds one.

The substations are unidirectional because of the rectifier. Consequently, a braking bus cannot send its energy back to the LVAC grid, but rather to other buses on the same section, or on a connected section. The first possibility for two sections to be connected is when they are supplied by the same substation: Bus 1 of Fig. 2, for example, can supply Bus 2 via the route FC1-substation busbar-FC2. The second possibility is when the sections are bilaterally connected. A bilateral connection is a controllable connection between two sections that are under different substations. The connection can be controlled as closed (connected) or open (isolated). Bus 2 can send power through the overhead lines to bus 3 as if sections 2 and 3 are one long section. Bus 1 can also share power with bus 3 via the route FC1-busbar-FC2-bilateral.

Finally, it is noticeable that each bus is connected to two lines in Fig. 2. In trolleygrids, an overhead return path for the current is also needed as the bus runs on wheels, unlike the tram which uses the rails as a return. In this paper, we define “supply zone” as the electrically connected zone in which a bus can send and receive power. Thanks to the bilateral connection, all the elements shown in Fig. 2 are part of one supply zone. The bus is supplied with the power to feed its traction and non-traction demands. When a bus is braking, in the absence of a receiving bus on the same supply zone or if the braking energy is excessive, the excess braking energy is wasted on-board in the braking resistors. The amount of energy wasted is controlled by a chopper circuit that controls the on-time of the resistors as to keep the grid voltage below the allowable upper limit (around 780 V, depending on the city). At values of around 720–740 V, also depending on the trolleygrid, the braking resistor is fully engaged to prevent any over-voltages.

To reduce the transmission losses on the section, an element found commonly in transport networks is the paralleled connection (or equipotential lines) between the overhead cables of the different bus lines on a section; i.e, the going and the returning traffic lines. Within the same section, the feed (positive) and the return (negative) lines are connected in pairs to offer a lower impedance path from the substation (or a braking bus) to the other bus loads. These lines are introduced periodically at a distance in the order of hundreds of meters (100–300 m).

2.2. Six methods for increasing the EV integration

To increase the integration potential of EV chargers, while respecting the grid limitations, this section studies six methods designed to tackle the power, voltage, and current limitations. This diverse set of proposed methods is important so as to offer a customized solution that can cater to the common violations at each substation. For example, short sections (a few hundred meters) would not typically see serious voltage drops in their short overhead cables and therefore do not benefit from a solution that primarily tackles the voltage drops. Table 3 summarizes the six methods and their intended mitigation use.

I **Substation level**

i *Increasing the substation nominal voltage*
This method increases the overall line voltage by increasing the substation no-load voltage setpoint via the traction transformer taps. This is not therefore a dynamic voltage-compensation method, but a one-time physical intervention. This method shifts the whole line voltage up, moving away from the critical voltage levels of 500 V and 400 V. Consequently, it also reduces the line current for the same power demand. A disadvantage is that the on-board braking resistor would be activated more frequently since the voltage is now closer to the upper limit of the grid. As a result, the total power consumption could be increased by this method, unless the reduction in transmission losses compensates for the loss in unharvested braking energy. This method invites the transport grid operators to rethink the substation no-load voltage set-points, not as a trade-off between braking energy harvesting and transmission losses, but also to take into account a desired minimum line voltage.

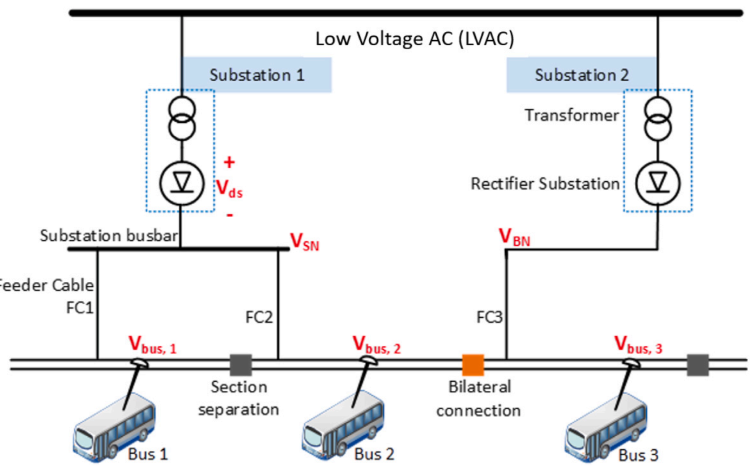

Fig. 2. The Trolleygrid and its components.

Table 3
Summary of the six methods addressed in this paper and their positive (+), negative (–), or neutral (o) effects on reducing the grid violations in power, voltage, and current, as well as their effect on the transmission losses and the braking energy recuperation.

	Reduces violations of:			Effect on:	
	Power	Voltage	Current	RI^2 losses	BR[a]losses
Higher Substation Voltage	+	++	+	+	–
Higher Substation Power Limit	++	0	0	0	0
Third paralleled Line	+	++	++	++	+
Bilateral Connection[b]	++	++	++	++	+
Fleet-Aware Smart Charging	++	++	++	+	++
Multi-port Converter	–	–	–	+	+

[a]Breaking energy recuperation.
[b]Unless both substations are heavily loaded.

In summary, as reported in Table 3, this method can directly reduce the voltage drops, and indirectly the power and current violations. This would reduce transmission losses, but has a negative effect on the braking energy recuperation (braking resistor activation).

ii *Increasing the substation power limit*
The substation power limit can be increased either by accepting a less conservative limit for the transformer overload or by an upgrade of the existing infrastructure to add capacity.
As reported in Table 3, while this method directly addresses the power violations, it changes nothing in the grid operation and power flow, however, and has therefore no effect on any other grid states or operations.

II **Grid infrastructure level**

i *Adding an extra overhead paralleled line*
The impedance in the overhead wires is effectively reduced by adding an extra overhead cable in parallel to the existing cables (typically two existing cables, one for each side of the road). Since the power flow solution is nonlinear (voltage source supply with power-source loads), this ratio in the reduction of the impedance would bring about an even more considerable reduction in the voltage drop than that ratio.
As reported in Table 3 then, this has a direct positive impact on current and voltage violations. Additionally, this has an indirect positive impact on power losses, and a more effective braking energy sharing, both of which lead to a reduction of the substation power demand.

ii *Introduction of a bilateral connection*
The introduction of a bilateral connection splits the section load supply to two different substations. As summarized in Table 3, this consequently reduces the line current, the line voltage drops, and the resistive losses. Additionally, it increases the effectiveness of braking energy sharing by more frequently exposing the braking vehicle to power-accepting nodes. Consequently, the power demand on each substation is lowered. It is worth noting still that this recuperation of the braking energy is only a passive benefit and, thereby, not the most effective solution.
On the other hand, due to the larger supply zone, faults in the system could occur more often per supply zone and influence a larger area, which is the main reason for the hesitation toward bilateral connections. Furthermore, it is worth noting that the power-sharing in a bilateral scenario is heavily influenced by the voltage of each substation [9].

III **EV charging level**

i *Introduction of a smart charging with a fleet-aware power management scheme*
Smart Charging controls the charging power continuously with respect to time [40–42]. With smart charging, the EV charging load could be reduced at moments when the loads are high, by measuring the instantaneous substation and fleet vehicles' powers and locations and wirelessly communicating them to the EV charger. With this, a power flow calculation (such as in [5,43,44]) can compute the voltage at every power node on the trolleygrid section, and the total power demand at the traction substation.

Based on this information, the allowed EV charging power is chosen at each instant as the maximum desired power that would not violate the local grid power, voltage, and current limitations such as those in Table 2 for the Dutch grid of Arnhem. The power output of the EV charger is determined from this calculation. This is referred to in this paper as Fleet-Aware Smart Charging and illustrated in Fig. 3.

In brief, an EV charger with a Fleet-Aware Smart Charging power management scheme receives the state (power, voltage, location, etc.) of each trolleybus and substation and load connected to a section. Then, implementing any readily available power flow calculation method from the literature calculates the maximum power it can draw at that instant that would not break any of the power, voltage, or current limitation of the local trolleygrid. This method is important because the small section lengths, moving loads, and severe voltage drops that can occur in transportation grids make the handling of EV chargers more complex than in regular distribution networks. An EV charger looking to maximize its power demand at a given instance needs to consider not only the available spare power capacity but also its effect on the line minimum voltage and maximum current for any vehicle on the section. For this, the EV charger's control algorithm should not only communicate with the supplying substation to compute the spare capacity (conventional smart charging). The controller needs to also communicate with all the moving vehicles of the fleet on the section to know their position and power demand, which is used to find the maximum allowable charging power that simultaneously respects the three grid limitations. The complexity of this method makes it hard to implement as it requires a lot of sensors, processors, and wireless communication between them. One alternative could be to use the available GPS bus data and the substation state (conventional smart charging) to estimate the state of each note on the grid, but that requires the development of a grid state estimator.

Another concern that can be raised is the Quality-of-Service (QoS) of EV charging. According to [45], the QoS can be examined on three levels: The energy delivered, the time of charging, and the variation of the charging power. However, the purpose of this method is to avoid the short moments of spare capacity dips that can occur on a trolley section, meaning that the charging is not significantly disturbed on a frequent basis. For example, a trolleybus acceleration lasts less than 10 s from 0 to its 300 kW peak [5], which means that the high power moments when the FASC method intervenes by curtailing the power is in the order of a few seconds. Furthermore, as seen in Fig. 1, the timetabling creates long periods of absolute zero-load on the traction substations where the QoS is fully ensured. The QoS is then not a significant concern with this method, especially with the rise of incentives such as in [46] that suggest payable schemes for users who require a perfect QoS.

By virtue of its design, this method is beneficial in all aspects as reported in Table 3. The only possible drawback can be that it is not as intensive in the reduction of losses as, for example, the bilateral connection since its function is to maximize the power drawn, and not reduce the losses. This maximization of the harvesting of the available power justifies why it is reported as having such a considerable effect on the braking energy recuperation.

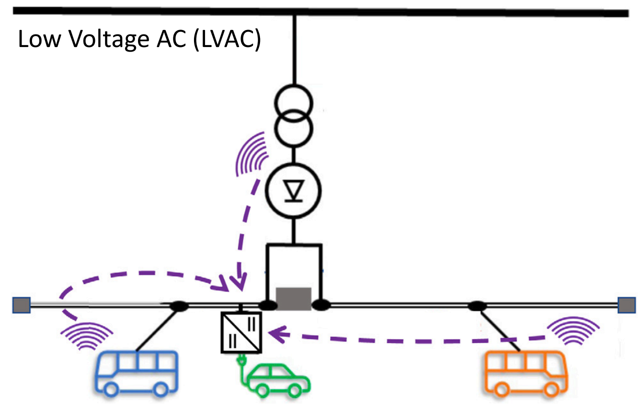

Fig. 3. Illustration of Fleet-Aware Smart Charging: In this method, the substation and the vehicles on the section communicate their states to the EV charger (power, voltage, location) and the latter computes its allowable charging power that would not break any of the grid limitations at any node on the line (not just at the charger).

ii *Introduction of a multi-port converter*

A multi-port converter (two inputs, one output) can be used to charge an EV from two separate traction substations. This is done by connecting each of the two input ports to a section of each substation. It is suggested as an alternative to a bilateral connection if a charger is desired near the section separation (end-of-line). In this manner, each substation is loaded with only half of the power demand of the EV charger. This is different from the bilateral case because only the charger is simultaneously fed from the two separate substations in this configuration and not the trolleybuses. This offers the charger the benefits of a bilateral connection without the related concerns for faults. This solution is further detailed and explored in [10].

The downside of this solution is that it can add more voltage, current, and power violations as it adds a load to the end-of-line of two sections. However, this method reduces the losses in supplying the converter when no buses are on the section (as shown in [10],) and increases the braking energy recuperation by harvesting it from two trolleygrid sections. The reported results are in Table 3.

3. Modeling methodology

3.1. Definition of the three case studies

This paper presents three case studies for EV integration. By choosing different grid parameters (grid layout, traffic, etc.), the cases help quantify and thereafter extrapolate the EV potential to various locations.

The three cases are:

- Supply zone T: Theoretical case study, as typically performed in literature, using a trapezoidal velocity profile on two very long sections (over 1200 m). The long section would mostly suffer from voltage problems
- Supply zone A: Case study from Arnhem with actual bus velocity and power data on two medium-to-long sections and with a low traffic
- Supply zone B: Case study from Arnhem with actual bus velocity and power data on two medium-to-short sections and with a high traffic

Table 4
Grid parameters were used for the theoretical study [5,8,16].

Theoretical grid parameters	Value	Unit
Total track length	4569	[m]
Section lengths	[1500; 1500; 1569]	[m]
Overhead line resistivity	172	[mΩ/km]
Feed-in point location	[0; 3000; 3000]	[m]
Feed-in cable length	[100; 100; 100]	[m]
Feed-in cable resistivity	56.6	[mΩ/km]
Substation Rated Power	[800; 800]	[kW]

Table 5
The characteristics of the supply zones investigated in the case study.

Supply zone	Substation & powering section(s)	$V_{nom,ss}$	Bilateral between sections
T	SS_1 = 111 SS_2 = 112 & 113	SS_1 = 650 V SS_2 = 650 V	111 & 112
A	SS_{12} = 23 & 24 SS_{13} = 2 & 3	SS_{12} = 686 V SS_{13} = 698 V	23 & 2
B	SS_9 = 25 SS_{14} = 26 & 27 & 41	SS_9 = 677 V SS_{14} = 628 V	25 & 26

Table 6
The characteristics of the sections where the EV chargers are placed for the case study.

Supply zone	Section	Length [m]	Feed-in point location [m]	Feed-in cable length [m]
T	111	1500	0	100
	112	1500	1500	100
A	23	850	80	98
	2	1300	1210	300
B	25	860	100	180
	26	650	550	70

The case studies are simulated for the worst-case scenario of high auxiliary demand (heating) and the highest traffic schedule (winter workday, day 268 in the year). The detailed information on all supply zones is in Tables 4, 5, and 6. From these, Table 7 alerts of the risks of violations at each supply zone as predicted by the key grid parameters [8].

In the theoretical study, Substation 1 is powering section 111, while Substation 2 is powering sections 112 and 113. The chosen parameters are based on typical trolleygrid parameters and summarized in Table 4. This section uses the same limitations and parameters previously described in Tables 2, 5, and 6.

3.2. Creating and quantifying a representative charging profile

For a representative EV charging power demand, two charging profiles are derived from measurements of 10,000 public charging transactions in The Netherlands in 2019 [47]. One charging profile is for the weekdays (7235 transactions), and the other is for the weekend days (2765 transactions). The charging profiles have a time step of 1 s. Fig. 4(a) provides an example of a few of the recorded 1000 transactions and Fig. 4 shows the resulting power distribution profile from the 10,000 transactions, normalized to a unity value. This unity demand is then multiplied by a constant factor to create the EV charging demand curve for the EV charger at any rated power in this study. As observed, the demand peak is around 9:00 during the weekdays and around 15:30 during the weekends.

From that, the number of EVs charged per day, referred to in this paper as # of EVs/day, is calculated by:

$$\text{\# of EVs/day} = \frac{\eta_{con} \cdot \eta_{EV}}{E_{batt}} \sum_{t=1}^{86400} P_{EV} \tag{1}$$

where: η_{con} is the DC/DC converter efficiency of the EV charger, assumed at 98%, η_{bat} is the battery charging efficiency, assumed constant at 95%, E_{batt} is the EV battery size of 60 kWh, and P_{EV} is the per-second charging power profile output of the studied scenario, summed over the 86,400 s of the day.

3.3. Trolleygrid power flow calculation

The trolleygrid power flow is calculated in per-second simulation steps using the comprehensive and verified simulation model previously detailed in [5]. This MATLAB model uses bus velocity and power input extrapolated from trolleybus measurements in the city of Arnhem and includes randomized traffic light and bus stop probabilities.

Important features of this grid model are that it accounts for bilateral connections and feeder cables. Another highlight of the model is that it models both the braking energy and the auxiliary demand of the trolleybus (mainly the heating and ventilation), which can be up to 50% of the bus power demand in harsh weather conditions [5,8,48]. The bus powers are given by Eq. (2). During braking, the bus power, P_{bus}, is the auxiliaries power P_{aux} plus the net exchanged with the grid P_{net} (obtained iteratively from the power flow calculation). The excess power, P_{BR}, is wasted in the braking resistors as demonstrated in Eq. (2).

While in traction mode, the bus power is simply the traction P_{tr} and the auxiliaries demand, P_{aux}.

$$P_{bus,j} = \begin{cases} P_{net,j} + P_{aux,j} + P_{BR,j} & \text{if braking} \\ P_{tr,j} + P_{aux,j} & \text{if traction} \quad j = 1..N_{bus} \end{cases} \tag{2}$$

The auxiliaries are –predominately– the HVAC load plus other base loads such as the on-board lights, screens, door motors, the control systems, etc.:

$$P_{aux} = P_{HVAC} + P_{base} \tag{3}$$

The HVAC energy requirement is calculated by a thermodynamic heat exchange model between the trolleybus and its surrounding environment, and is detailed in [5].

From this energy requirement, the HVAC power is derived. For the Arnhem bus types, the HVAC system is controlled with a duty cycle (t_{cycle}) of 5 min. The on-time, t_{on}, of the HVAC system for each period is dictated by the HVAC energy requirement during that cycle:

$$t_{on} = t_{cycle} \frac{\overline{P_{HVAC}}}{P_{rated}} \tag{4}$$

where $\overline{P_{HVAC}}$ is the average power requirement in the 5 min and P_{rated} is the nominal HVAC power, namely 36.5 kW for the Arnhem system. Finally, in this paper, P_{base} is taken as 5 kW as an estimate provided from the Arnhem trolleybus measurements [5,48].

The nodal model is based on the forward–backward sweep convergence logic, where each load (trolleybus or EV charger) is considered a node. The model's output is, among others, the voltage and power at every node, the branch currents, and the losses. This provides the data needed for the detailed analysis of the grid violations. The braking energy is treated as follows: First, the model runs until power-balance convergence. Second, the model checks to see if the substation current solution is a negative number (excess braking energy) and/or if the bus voltage is above the braking resistor limit (740 V for Arnhem). If so, the regenerative bus power is curtailed by the "unacceptable" power amount, which is the substation voltage times the negative current and/or the bus voltage above 740 times the bus current. Then, the iteration is repeated, and this process in general, is repeated until the results are acceptable. This is admittedly a slow convergence method where the curtailment is in the order of a few kWs at each step. Still, it robustly approaches the actually used bus power without overshooting it since the non-linearity of the power flow makes it hard to directly estimate the used braking energy and transmission losses from an analytical power balance. The only computationally-fast exception is when a braking bus is alone on the section (no load), so all the braking energy is immediately wasted. The final modeling flowchart is presented in Fig. 5.

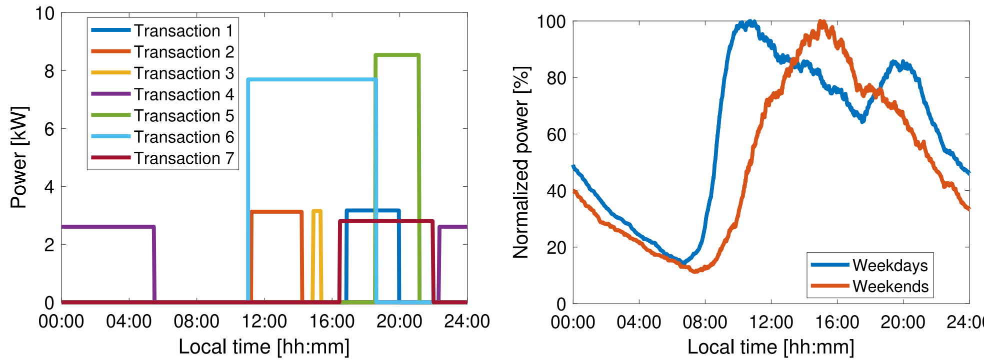

(a) Various charging transactions. (b) EV power profile distribution over a day.

Fig. 4. The EV charging demand used in this paper from 1000 measured transactions in [47], (a) example of a few measured transactions, (b) summation curve of the 1000 transactions, normalized to a unity value.

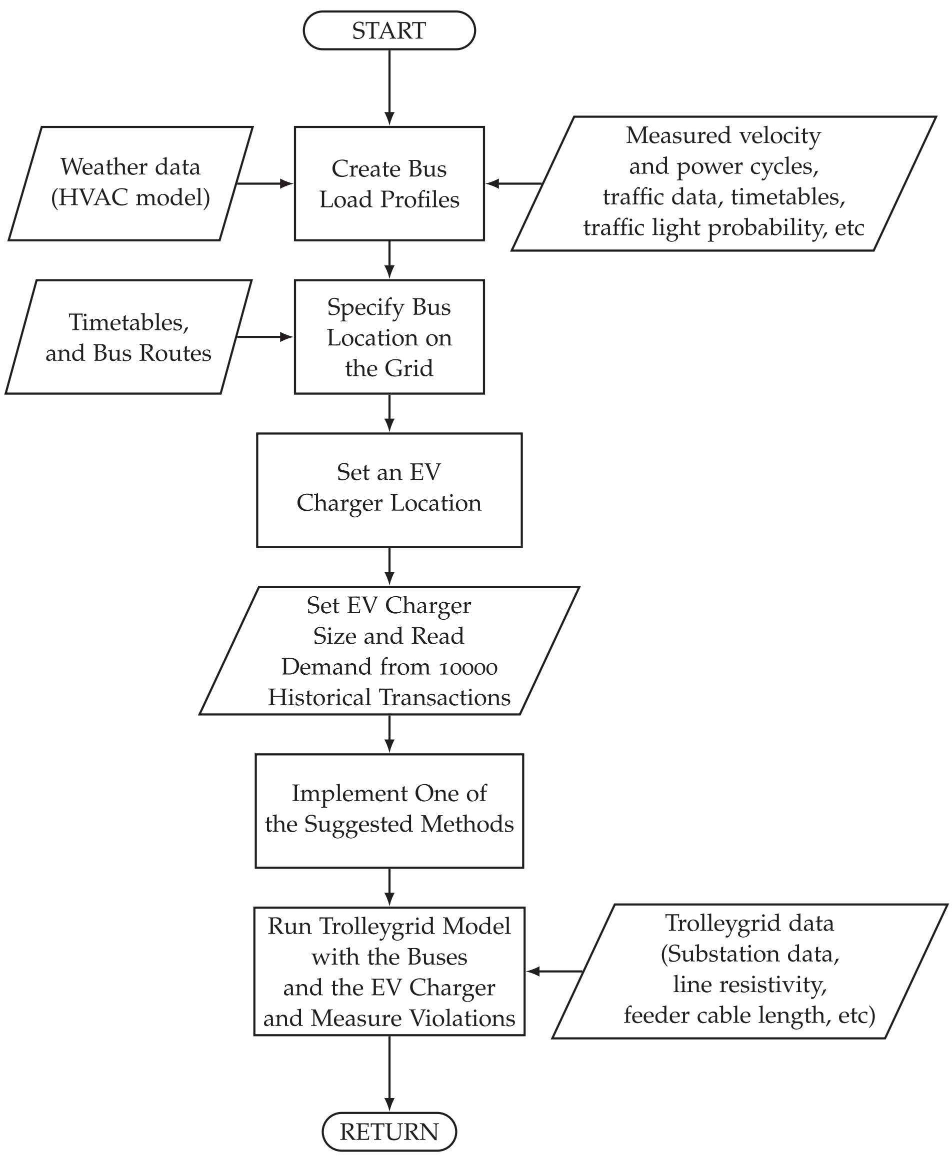

Fig. 5. Flowchart of the trolleygrid model with the EV charger.

Table 7
Risk of violations at each supply zone from key grid parameters.

	Effect on violations	Risk at supply zone		
		T	A	B
Section Length	V, I	High	Medium	Low
SS Nominal Voltage	V, I	High	Low	Medium
Average Traffic	P, V, I	Medium	Medium	High
Peak Traffic	P, V, I	Low	Medium	High

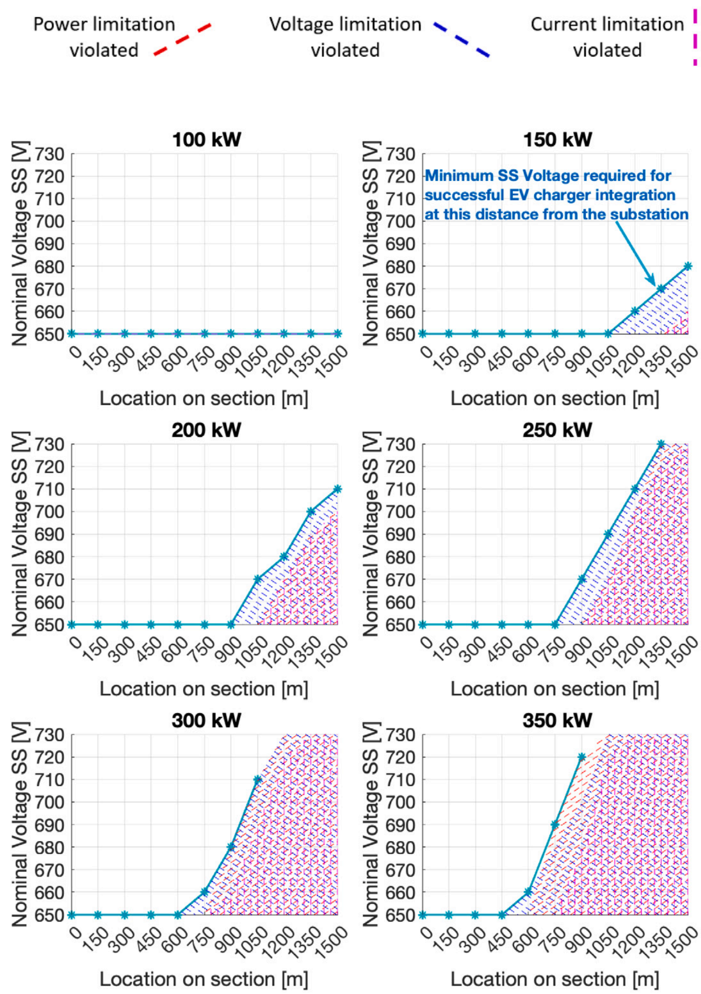

Fig. 6. The minimum substation voltage required for the successful EV charger integration of a certain size at any location on the section. The zone and type of the limiting grid violations are shown with dashed lines.

4. Theoretical grid case study

The purpose of this section is to present the results of the case study of a theoretical grid, as is commonly approached in literature. This study will highlight the impact of the six methods on long sections of low substation voltage and low, yet constant traffic. Along with the case study of the Arnhem trolleygrid in the section, this offers generalized results by looking at different infrastructure topologies and bus traffic intensity.

4.1. A closer look at some results: Higher substation nominal voltage

Substation voltages are typically designed as a trade-off between the minimum line voltage and the facilitation of regenerative braking energy sharing between far buses [8,9,21,49]. A section with a low substation voltage cannot allow EV charger integration as it would quickly experience voltage (and consequently power and current) violations. Such sections benefit from higher substation voltages and offer a smart base load that would still allow efficient harvesting of the regenerative braking energy.

The effects of this method are observable in Fig. 6, showing the minimum substation voltage required to allow the EV charger integration at any location on the section, and the grid violations that limit if the substation voltage is lower.

For example, In the case of a 200 kW charger, an EV charger of this size can only be implemented at 1050 m from the substation if the substation voltage is at least 670 V. Otherwise, the simulations have shown that there would be voltage violations (blue dashed zone in the figure). Meanwhile, this charger at 300 m from the substation could still be feasible with as low as 650 V. On the other hand, a 350 kW charger at 1050 m from the substation cannot be guaranteed with a simple tuning of the substation voltage (the teal-blue curve is discontinued). As the figure shows, this is because there is a power violation at this

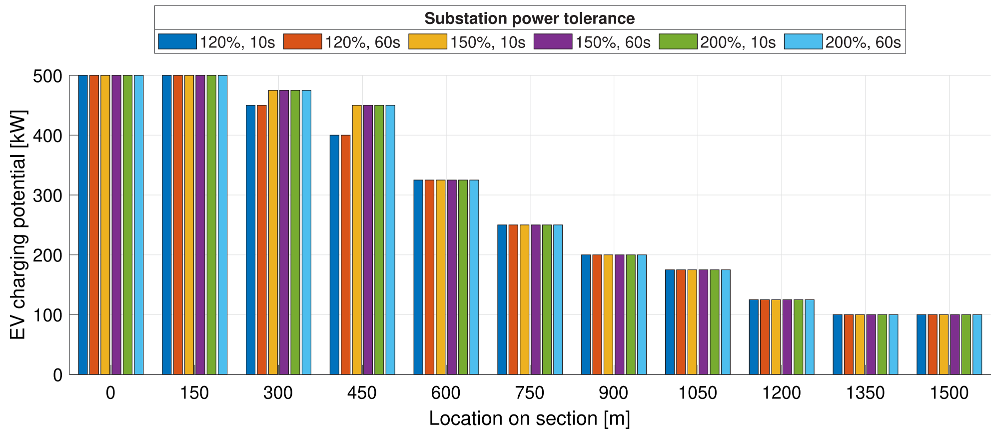

Fig. 7. Effect of various maximum substation power tolerances on the EV charging potential for section 111 for different charger locations: [Multiple of substation rated power, continuous violation duration].

charger size (red dashed zone) that a mere voltage upgrade cannot solve.

The 100 kW charger is feasible anywhere on the section. However, as these two long sections have a relatively low substation voltage, it is expected that the voltage is indeed the limiting factor for chargers up to 250 kW far from the feed-in point. For 300 kW and 350 kW, power violations become the limiting factor, which is expected as these large values are almost half of the rated substation power of 800 kW. Tuning the nominal voltage of a substation to a higher level is indeed an effective solution, especially at the end-of-line (EOL) of a long section of low, yet constant traffic.

4.2. A closer look at some results: Higher substation power limit

The effects of this method are observable in Fig. 7, showing the effect of various maximum substation power tolerances on the EV charging potential for section 111 for different charger locations along the section. The simulated values are shown as [Multiple of substation rated power, continuous violation duration], for example, as [120%, 10s] to show that the power demand at the substation is tolerated to go as high as 120% of the rated power for 10 consecutive seconds. No considerable benefit, if any, is brought on by changing the substation power limit in this section. These results were expected as long sections of low, yet constant traffic do not have a more pronounced voltage problem than a power problem. Consequently, accepting a more lenient power peak tolerance would do little, if any, to increase the potential for EV integration.

4.3. A closer look at some results: Fleet-aware smart charging

Figs. 8(a) and 8(b) display the different loads on the section when a 500 kW EV charger is placed at 400 meters from the feed-in point with a ramp-up/down speed of 3 kW/s and 9 kW/s, respectively.

The ramping up and down is activated when the EV charger detects a rise or drop, respectively, in the available spare capacity. The ramping is helpful from a stability perspective to avoid harsh fluctuations on the line from the chargers connecting/disconnecting in full. This allows the charger to follow the spare capacity trend in a smooth fashion and account for the delays in the telemetry and the processing time of the data used to compute the spare capacity.

As seen in the figures, the higher ramp-up/down converter can respond faster to various bus loads, with better peak shaving as a result. Such an example can be best offered at 9:05 when the violating power peak at 3 kW/s is avoided at the 9 kW/s scenario. Still, more examples can be observed in multiple power peaks, albeit non-violating, being shaved.

4.4. Overview of the six grid methods — Theoretical study

The previous subsections provided a closer look and a detailed analysis of three methods. The results of all six methods for the theoretical supply zone are summarized in Fig. 9 and Table 8 summarizes the numerical results for all the grid methods. As expected, the long, low-traffic sections 111 and 112 are restrained by the voltage limitation when it comes to the integration of additional load.

Consequently, the voltage-oriented solutions of higher SS voltage, extra paralleled line seem more effective–especially at EOL (end of line)–, as well as the bilateral connection, which seems even more effective at MOL (mid of line) in addition to the EOL. Meanwhile, the power-oriented solution of increasing the substation limit has no noteworthy benefit. Furthermore, the multi-port converter (two inputs, one output) offers less potential for EV charging compared to the baseline. This is an inherent consequence of its end-of-line placement and of the voltage drops that it brings to both sections to which it is connected.

On the contrary, the smart charging method produces the highest benefit at the SOL (start of line) of both sections, while its benefit is less pronounced at MOL/EOL for section 111, and EOL of 112.

This can be explained by the fact that the fleet-aware smart charging only looks for harvesting the *attainable* charging power available, without increasing the spare capacity of the substations in any way. As both sections have very low traffic (read: power demand), there is a lot of spare capacity whenever smart power management is involved.

However, there is no active management solution that would help the limiting voltage drops at the EOL, and those need a passive solution that boosts the voltage altogether, such as substation voltage, paralleled lines, bilateral connections, or a combination of these.

The MOL advantage of 112 is that this section is powered along with another section (namely 113,) by one substation. This gives the advantage to the Smart Charging method as it has all the necessary information at the substation level, not only the section level.

This information is hidden from the other, mostly-passive methods, that only have local, section-level information. This is why with section 111, powered alone by a substation, this all-knowing advantage of the Fleet-Aware smart charging method disappears at the MOL.

5. Arnhem grid case study

5.1. A closer look at some results: paralleled lines

5.1.1. Supply zone A

Fig. 10 shows the EV charging potential for two paralleled overhead lines (baseline scenario) and three paralleled overhead lines. The EV charging potential is 25 kW higher for most locations on section 23.

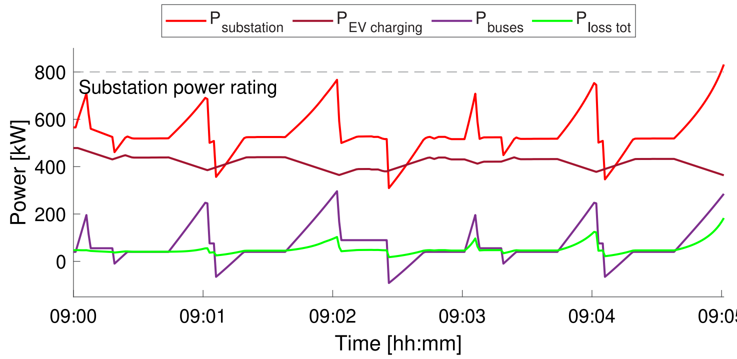

(a) Loads on section 111 with a ramp-up/down speed of 3 kW/s.

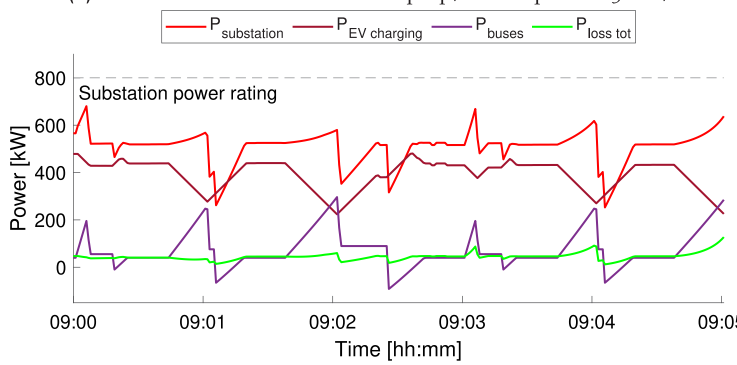

(b) Loads on section 111 with a ramp-up/down speed of 9 kW/s

Fig. 8. The substation power (buses + EV + line losses) for an EV charger at 400 m. It is noticeable at 9:05 that the faster response of the management system allows the grid to avoid a power violation that occurs with the slower response.

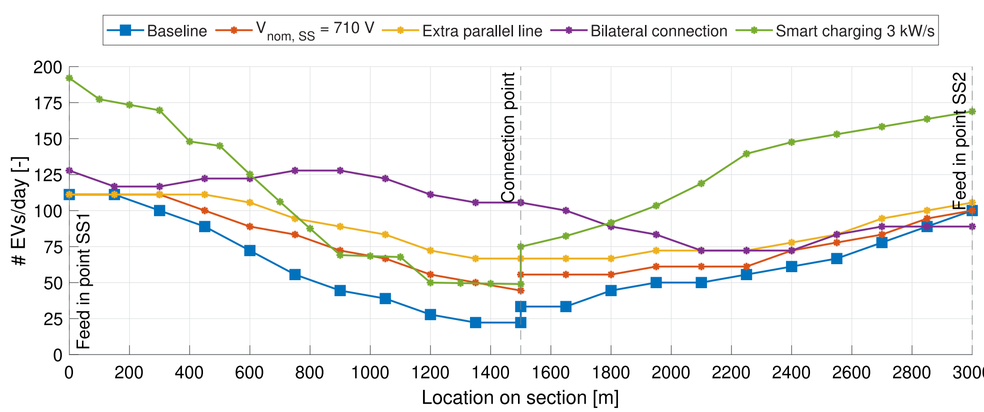

Fig. 9. Summary of various grid methods on the maximum achievable EV charging potential on the theoretical sections 111 (left) and 112 (right). Grid methods: increasing substation power and the multi-port converter are excluded from this graph as they showed no benefit.

Table 8
Supply zone T: effect of grid methods on the maximum achievable EV charging potential in the theoretical study.

Grid method	Section 111 [# of EV/day]		Section 112 [# of EV/day]		Sec. 111+112 [# of EV/day]
	Max.	Mean.	Max.	Mean.	Max.
Baseline	111	63	100	60	211
Increasing voltage	111 (+0)	81 (+18)	100 (+0)	71 (+11)	211 (+0)
Substation power	111 (+0)	65 (+2)	111 (+11)	74 (+14)	222 (+11)
Extra overhead line	111 (+0)	93 (+30)	106 (+6)	80 (+20)	217 (+6)
Bilateral connection	128[a] (+17)	119[a] (+56)	106[a] (+6)	86[a] (+26)	128[a] (−83)
Fleet-aware smart charging	182 (+71)	110 (+47)	167 (+67)	126 (+66)	349 (+138)
Multi-port converter	22 (−89)	0 (−63)	33 (−67)	0 (−60)	56[b] (−155)

[a]Achievable with one charger.
[b]Achievable with one charger at the connection point.

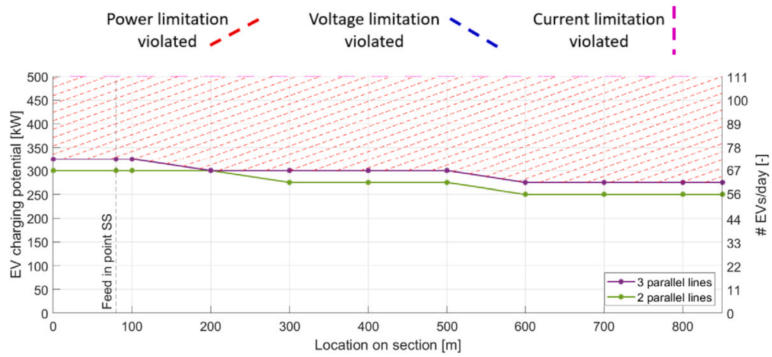

Fig. 10. Effect of adding extra paralleled overhead wire on the maximum achievable EV charging potential on section 23, day 268. The colored area indicates the limiting factor in the three paralleled overhead wire scenario.

Table 9
Section 23: comparison of energy consumption substation and transmission losses with an extra paralleled line. The size of the EV charger is the maximum potential in that specific location for the two paralleled line case.

Location	EV charger	E_{SS} [kWh/day]		$E_{loss,trans}$ [%]	
[m]	[kW]	2 lines	3 lines	2 lines	3 lines
0	300	4970	4959 (−0.22%)	0.89	0.68 (−23.6%)
200	300	4987	4970 (−0.34%)	1.24	0.90 (−27.4%)
400	275	4686	4649 (−0.79%)	2.53	1.75 (−30.8%)
600	250	4365	4313 (−1.19%)	3.57	2.41 (−32.5%)
800	250	4424	4350 (−1.67%)	4.85	3.23 (−33.4%)

With the introduction of an extra paralleled line, the power rating of the substation is still the limiting factor. In contrast to the results found in the sections of the theoretical study, the substation power tolerance is the limiting factor on this section and not the minimum line voltage. Therefore, the effect of this method is negligible. Adding an extra paralleled reduces the substation power slightly by reducing the transmission losses, and increases the EV charging potential. But the effect of the reduction on the voltage drop is more significant, as shown in the case study, and this method should be used in such environments. Table 9 summarizes the energy savings associated with introducing the additional paralleled overhead line. This method has the highest effect on the reduction of the energy consumption of the substation when placing the EV charger further away from the feed-in point (EOL). With a 250 kW EV charger, adding an extra paralleled line reduces the energy use by 74 kWh/day. This is −1.67% of the SS energy, but 33.4% of the transmission losses.

5.1.2. Supply zone B

Fig. 11 shows the EV charging potential for two paralleled overhead lines (baseline scenario) and the three paralleled overhead lines scenario. Depending on the location of the EV charger, the potential increases between 25 and 50 kW. This is expectedly similar to the results of supply zone A because the substation power limitation is the limiting factor here as well.

5.2. A closer look at some results: Introducing a bilateral connection

5.2.1. Supply zone A

In supply zone A, a bilateral connection between sections 23 and 2 is possible. Substation 12 is powering sections 23 and 24, whereas substation 1 is powering sections 2 and 3. The substation nominal voltages are 686 V and 698 V, respectively. The effect of this grid method is shown in Fig. 12. In the bilateral connected scenario, the maximum EV charging potential is between the connection point and substation 13. In this region, substation 13 supplies most of the power to the charger. The colored area indicates the limiting factor for the bilateral case.

5.2.2. Supply zone B

Due to the relatively significant difference of $V_{nom,\ SS}$, 677 V vs. 628 V, the introduction of the bilateral changes the power source for the trolleybuses and EV chargers in supply zone B [9]. For the baseline simulation, the EV charging potential on section 26 is zero at every location, as seen in Fig. 13. With the bilateral connection between sections 25 and 26, substation 9 can power section 26. Therefore, the loads on section 26 can be also served by substation 9, and more EV potential can be created.

However, the EV charging potential decreases at some point on section 25. Fig. 14 shows the energy shared between the two substations on supply zone B when an EV charger of 100 kW is integrated on the sections. Due to the higher nominal voltage of substation 9 compared to substation 14, most of the supplied power is supplied by substation 9 [9].

5.3. A closer look at some results: Multi-port converter

A Multi-port converter between 25 and 26 would not be feasible, as section 26 has no power capacity. The EV charging potential at the connection point of the sections is then 0 kW. This highlights the key difference between a multi-port and a bilateral connection, in how the multi-port brings to the grid the disadvantages of the EOL placement (lower voltages and higher line currents), while bringing none of the benefits of the bilateral connection. Indeed, as is presented later, a bilateral connection does create an EV charging potential at section 26.

5.4. Overview of the six grid methods — Arnhem case studies

The previous subsections provided a closer look and a detailed analysis of three methods. Figs. 15 and 16 and Tables 10 and 11 summarize the results of the six proposed methods as well as a combination of the capacity-building increasing ones (case 1): $V_{nom,\ SS}$ = 710 V, an extra paralleled overhead line, and a substation power rating of 1100 kW. The 1100 kW is 300 kW more than the current limit of 800, and that

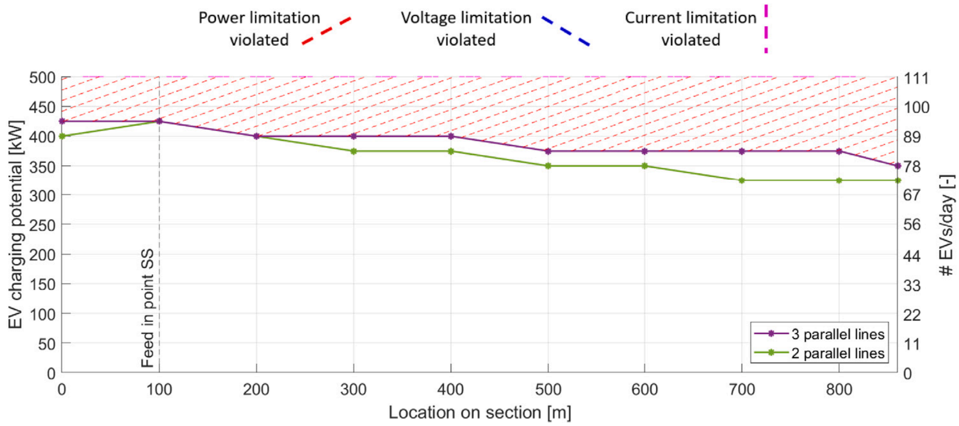

Fig. 11. Effect of adding extra paralleled overhead wire on the maximum achievable EV charging potential on section 25, day 268. The colored area indicates the limiting factor in the three paralleled overhead wire scenarios.

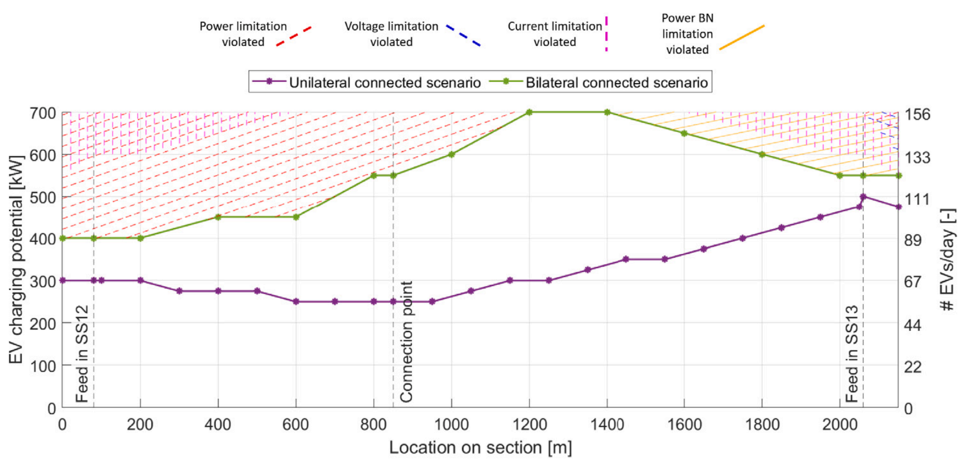

Fig. 12. Effect of introducing bilateral connections between sections 23 (left, 0–850 m) and 2 (right, 850–2150 m) on the maximum achievable EV charging potential.

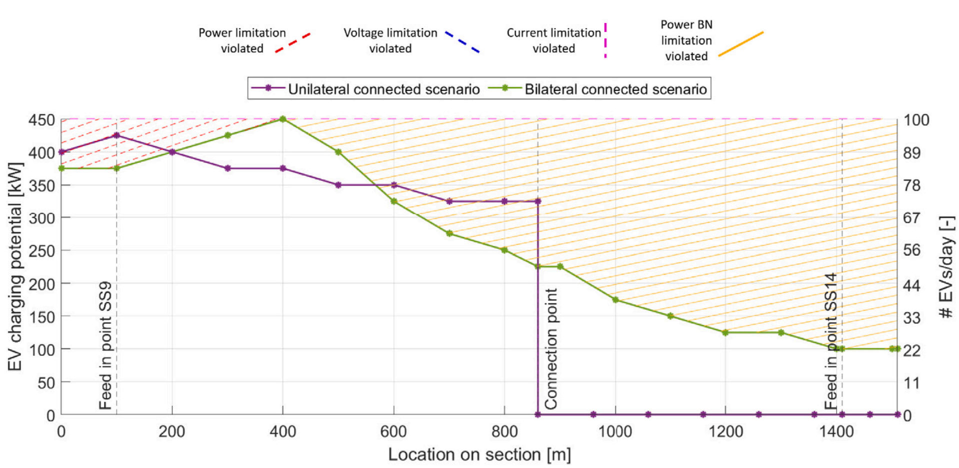

Fig. 13. Effect of introducing bilateral connections between sections 25 (left, 0–860 m) and 26 (right, 860–1510 m). The power limitation at the bilaterally connected substation P_{BN} is also shown.

is the power of one accelerating bus with the heating system on.

In supply zone A, section 23 is medium length with a medium-high substation voltage and thereby did not have a voltage or line current problem. It is expected then that the substation voltage and extra paralleled line methods do not contribute to any benefit, while the other power-centric methods did.

By contrast, section 24 is a long section supplied by a substation that is feeding another long section. While the traffic is medium in average-values and peak-values on the section, its connection to another long section of similar traffic means there are many instances of low spare grid capacity (as opposed to short sections that do not see a bus traffic for long). This explains why the static power solutions of "Case 1" and "increasing the power limit" did not offer much additional potential to

Table 10
Supply zone A: effect of grid methods on the EV charging potential for the case study on day 268 of the year.

Grid method	Section 23 [# of EV/day]		Section 2 [# of EV/day]		Section 23+2 [# of EV/day]
	Max	Mean	Max	Mean	Max
Baseline	67	61	111	82	178
Increasing voltage	72 (+5)	63 (+2)	111 (0)	83 (+1)	183 (+5)
Substation power	111 (+44)	103 (+42)	111 (0)	96 (+14)	222 (+44)
Extra overhead line	72 (+5)	66 (+5)	111 (0)	94 (+12)	183 (+5)
Bilateral connection	122[a] (+55)	103[a] (+42)	156[a] (+45)	137[a] (+55)	156[a] (−22)
Fleet-aware smart charging	114 (+47)	108 (+47)	201 (+90)	178 (+96)	315 (+137)
Multi-port converter	56 (−11)	0 (−61)	56 (−11)	0 (−82)	111[b] (−67)
Case 1	150 (+83)	115 (+54)	161 (+50)	109 (+27)	311 (+133)

[a]Achievable with one charging facility.
[b]Achievable with one charging facility at the connection point of the sections.

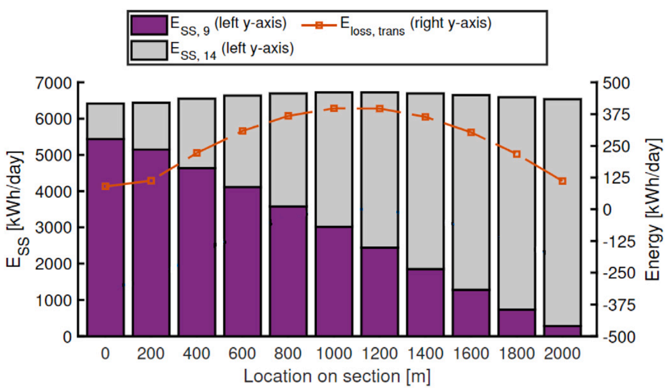

Fig. 14. Energy share of the two substations in supply zone A (left axis). A 400 kW EV charger is placed at different locations on sections 23 and 2. The orange line (right axis) shows the cables' energy losses due to transmission losses. (For interpretation of the references to color in this figure legend, the reader is referred to the web version of this article.)

the section as did the "load-shifting" methods of smart charging and bilateral connection. In short, this section had a lot of spare capacity once the load (especially the peaks) could be shifted or shared, rather than a fixed increase in power capacity. Interesting also to note that as this section is long, the extra line had a clear positive impact at EOL.

Supply zones B clearly had a power problem, especially section 26. It was expected that voltage and current methods do not produce tangible benefits.

Two interesting phenomena appear in these results. The first is that, unlike supply zone A, section 26 did not benefit from smart charging. This is explained by the fact that this overloaded section (high traffic, connected to a substation that feeds 3 sections) does need a fixed increase in capacity. Here, the bilateral method, increase of substation limit, and Case 1 create an EV charging potential that did not exist.

The other interesting phenomenon is that the introduction of a bilateral connection showed a decrease in the EV potential at some locations on 25. This is to be expected as the bilateral connection coupled to section 25 with section 26 which had no spare capacity and is of a much lower substation voltage. Therefore, section 25 had to supply many of loads of substation 26.

6. Recommendations for increasing method, placement, and sizing of EV chargers in public transport networks

The results of the previous sections offer insights into the best method to increase the EV chargers integration, placement, and sizing, for an array of different transport grid landscapes.

6.1. Suggestions for the choice of the potential-increasing method

- Increasing the substation voltage: This method is best suited for an EV charger placement at the EOL of long, low average traffic, low peak traffic sections. Otherwise, there is no mentionable benefit. This can be seen in detail in the results of Section 4.1.
- Introduction of an extra paralleled line: This method has the same suggestions as the above one. It is worth mentioning, however, that increasing the substation voltage is an effectively cost-less solution, and is therefore preferred over this method. This can be seen in detail in the results of Section 5.1.
- Increasing the substation power limit: This method is most effective for locations with medium to high average traffic densities. If the traffic congestion happens in peaks only, it is better to go for instantaneous relief solutions, such as Fleet-Aware Smart Charging, rather than increasing the substation capacity. This can be seen in detail in the results of Section 4.2.
- Fleet-Aware Smart Charging: This method is always a good solution to draw the available grid power for the EV chargers. Trivially, it is not beneficial in locations of high average and peak traffic intensities, as these locations have no spare capacity to be harvested. This method only harvests the attainable spare capacity but does not *create* any compared to the baseline, as is the case with a bilateral connection or the addition of a paralleled line, for example. The main advantage of this method shows up at sections that are supplied by a substation that feeds multiple sections, as this method, by its sensors and communication, can actively avoid violating the grid limits. However, this method is expensive (sensors) and requires reliable wireless communication. This can be seen in detail in the results of Section 4.3.
- Introduction of a bilateral connection: This method is best suited at the MOL and EOL of long sections, but has an overall visible benefit at almost any location. The only exception is when placing an EV charger on a section that is then bilaterally connected to a section with no spare capacity, as this would cause a reduction of the local spare capacity since a part of it goes to its neighboring section (case study of supply zone B). This can be seen in detail in the results of Section 5.2.
- Use of a multi-port converter: Unfortunately, this method is not recommended as it always produced results lower than the baseline. The reason the MPC has a poor performance is that it presents to the grid all the disadvantages of a load at the EOL (more severe voltage drops and higher currents and losses), without any of the benefits of a bilateral connection since the vehicle loads on the two sections are still galvanically isolated. This can be seen in detail in the results of Section 5.3.

6.2. Suggestions for the sizing of EV chargers

There is a charging potential for 150–200 EVs per day anywhere along long sections of medium-to-low traffic that are fed alone or with

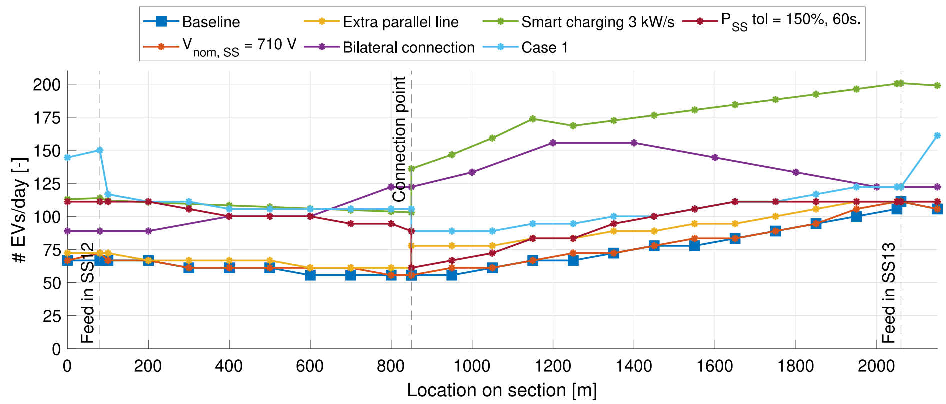

Fig. 15. Summary of various methods on the maximum achievable EV charging potential in supply zone A sections 23 and 2 on day 268. Case 1: $V_{\text{nom, SS}}$ = 710 V, an extra paralleled overhead line is added to the section, and the substation power rating is increased to 1100 kW.

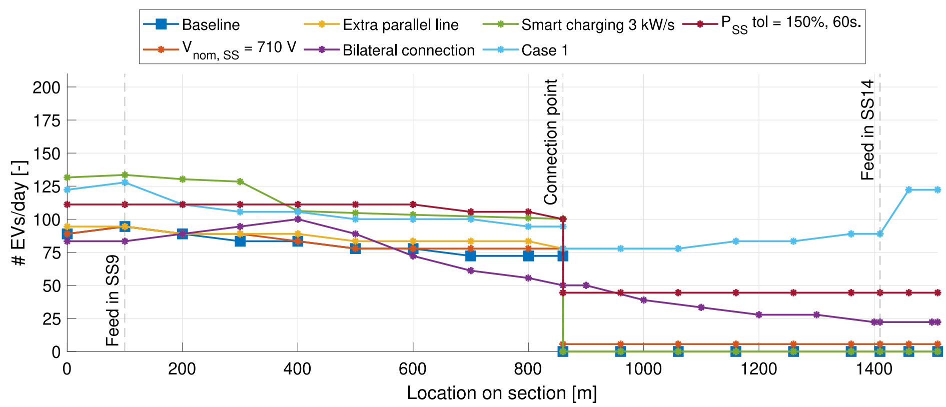

Fig. 16. Summary of the effect of various methods on the EV charging potential in supply zone B sections 25 and 26. Case 1: $V_{\text{nom, SS}}$ = 710 V, an extra paralleled overhead line is added to the section, and the substation power rating is increased to 1100 kW.

Table 11
Supply zone B: effect of grid methods on the EV charging potential for the case study.

Grid method	Section 25 [# of EV/day]		Section 26 [# of EV/day]		Section 25+26 [# of EV/day]
	Max	Mean	Max	Mean	Max
Baseline	94	81	0	0	94
Increasing voltage	94 (0)	83 (+2)	6 (+6)	6 (+6)	100 (+6)
Substation power	111 (+17)	109 (+28)	44 (+44)	44 (+44)	156 (+62)
Extra overhead line	94 (0)	87 (+6)	0 (0)	0 (0)	94 (0)
Bilateral connection	100[a] (+6)	78[a] (−3)	50[a] (+50)	30[a] (+30)	100[a] (+6)
Smart charging	134 (+40)	114 (+33)	0 (0)	0 (0)	134 (+40)
Multi-port converter	72 (−22)	0 (−81)	0 (0)	0 (0)	72[b] (−22)
Case 1	128 (+34)	106 (+25)	122 (+122)	91 (+91)	250 (+156)

[a]Achievable with one charging facility.
[b]Achievable with one charging facility at the connection point of the sections.

one other section from their substation, as long as it is with the fleet-aware smart charging method. It is also possible at MOL and EOL of long, medium-to-low traffic sections that are bilaterally connected to another mid-to-low traffic section. Care should be considered at the SOL of very long sections that are supplied by a substation that feeds multiple sections, as only the smart charging method could prove beneficial, and for a low EV charging potential of about 75 EVs per day. Care is also advised at MOL of high average and peak traffic densities that are supplied by a substation that feeds multiple sections, as the EV charging potential is also limited. This is because the MOL sees a lot of violations as it has neither the benefit of being close to the feed-in point, nor that of being close to the EOL and the bilateral connection.

6.3. Suggestions for the placement of EV chargers

EV chargers are placed where there is parking spot and a need for a charger. However, when the placement offers some flexibility, the following recommendations are presented:

- Place the EV charger at SOL when implementing Fleet-Aware Smart Charging, except at sections with high average and peak traffic densities that are supplied by a substation that feeds multiple sections. In that case, SOL is advised with a bilateral connection or increasing the substation power capacity.
- Place the EV charger at MOL when implementing fleet-aware smart charging or a bilateral connection at long, medium average and peak traffic sections. Avoid the MOL placement at sections

with high average and peak traffic densities that are supplied by a substation that feeds multiple sections, for the reasons previously explained.
- Place the EV charger at EOL for long, medium-to-low average and peak traffic sections that are supplied by a substation that feeds multiple sections, when adding a bilateral connection. These sections have voltage and power violations, and benefit the most from a bilateral connection

7. Conclusions and future works

This paper presented six methods for increasing the integration potential of EV chargers in electric public transport grids, assessed their benefit, and offered recommendations on the placement and sizing.

In conclusion, there is no single solution that fits all types of sections and their parameters (length, average traffic, peak traffic, etc.). For this purpose, Section 6 offers a detailed, tailored suggestion for each method, sizing, and placement option.

However, some general conclusions can still be made regardless of the specific grid layout or size and location of the EV charger. For example, the multi-port converter (two inputs, one output) was found to be worse than the baseline, regardless of the case study, as it presented to the grid all the disadvantages of a load at the end-of-line of two sections (more severe voltage drops and higher currents and losses), without any of the benefits of a bilateral connection.

The bilateral connections are the most beneficial and cost-efficient solution in all cases except for a section coupled with an already congested section. This is because no spare capacity could be provided in that case. On the contrary, in the case study of supply zone B, the combined spare capacity dropped compared to the baseline since the congested section was exploiting the spare capacity of the uncongested section.

Fleet-Aware Smart Charging with sensors and wireless communication can increase the potential significantly by continuously sensing and analyzing the grid states to avoid grid violations. It is a costly and complex solution. This is because it requires sensors at each trolleybus, substation, and power load, as well as wireless communication between them and the EV charger that processes the data and finds the allowed instantaneous charging power that would not violate the grid power, voltage, or current limits neither at the EV charger nor any other node on the section. Furthermore, this method is only suitable for sections with a spare capacity since Fleet-Aware Smart Charging only harvests the available capacity but does not create any.

Future work is needed in testing more combinations of grid methods and quantifying their effects. More urgently, a cheaper yet reliable method of estimating the grid states is crucial to harvest the outstanding benefits of Fleet-Aware Smart Charging with sensors, but without the costs and complexity of such an added infrastructure.

CRediT authorship contribution statement

Koen van der Horst: Data curation, Methodology, Investigation, Software, Validation, Visualization, Writing – original draft. **Ibrahim Diab:** Conceptualization, Formal analysis, Methodology, Investigation, Software, Validation, Visualization, Writing – original draft. **Gautham Ram Chandra Mouli:** Supervision, Writing – review & editing, Project administration, Funding acquisition. **Pavol Bauer:** Supervision, Writing – review & editing, Project administration, Funding acquisition.

Declaration of competing interest

The authors declare the following financial interests/personal relationships which may be considered as potential competing interests: Ibrahim Diab reports financial support was provided by Electric Mobility Europe.

Data availability

Data will be made available on request.

Acknowledgment

This research was funded by the Trolley2.0 project of Electric Mobility Europe.

References

[1] Unterluggauer T, Rich J, Andersen PB, Hashemi S. Electric vehicle charging infrastructure planning for integrated transportation and power distribution networks: A review. ETransportation 2022;100163.
[2] Rahman S, Shrestha G. An investigation into the impact of electric vehicle load on the electric utility distribution system. IEEE Trans Power Deliv 1993;8(2):591–7.
[3] Khalid MR, Alam MS, Sarwar A, Asghar MJ. A comprehensive review on electric vehicles charging infrastructures and their impacts on power-quality of the utility grid. ETransportation 2019;1:100006.
[4] Gruosso G, Mion A, Gajani GS. Forecasting of electrical vehicle impact on infrastructure: Markov chains model of charging stations occupation. ETransportation 2020;6:100083.
[5] Diab I, Saffirio A, Mouli GRC, Tomar AS, Bauer P. A complete DC trolleybus grid model with bilateral connections, feeder cables, and bus auxiliaries. IEEE Trans Intell Transp Syst 2022;1–12. http://dx.doi.org/10.1109/TITS.2022.3157080.
[6] Bartłomiejczyk M. Practical application of in motion charging: Trolleybuses service on bus lines. In: 2017 18th international scientific conference on electric power engineering. 2017, p. 1–6. http://dx.doi.org/10.1109/EPE.2017.7967239.
[7] trolley:motion. Trolley:motion. 2020, https://www.trolleymotion.eu/.
[8] Diab I, Scheurwater B, Saffirio A, Chandra-Mouli GR, Bauer P. Placement and sizing of solar PV and wind systems in trolleybus grids. J Clean Prod 2022;131533.
[9] Diab I, Mouli GRC, Bauer P. Increasing the integration potential of EV chargers in DC trolleygrids: A bilateral substation-voltage tuning approach. In: 2022 international symposium on power electronics, electrical drives, automation and motion. 2022, p. 264–9. http://dx.doi.org/10.1109/SPEEDAM53979.2022.9841989.
[10] Shekhar A, Mouli GCR, Bandyopadhyay S, Bauer P. Electric vehicle charging with multi-port converter based integration in DC trolley-bus network. In: 2021 IEEE 19th international power electronics and motion control conference. IEEE; 2021, p. 250–5.
[11] Diab I, Saffirio A, Chandra-Mouli GR, Bauer P. A simple method for sizing and estimating the performance of PV systems in trolleybus grids. J Clean Prod 2023;384:135623.
[12] Iannuzzi D, Lauria D, Tricoli P. Optimal design of stationary supercapacitors storage devices for light electrical transportation systems. Opt Eng 2012;13(4):689–704.
[13] Rufer A, Hotellier D, Barrade P. A supercapacitor-based energy storage substation for voltage compensation in weak transportation networks. IEEE Trans Power Deliv 2004;19(2):629–36.
[14] Zhang D, Jiang J, Zhang W, et al. Robust and scalable management of power networks in dual-source trolleybus systems: A consensus control framework. IEEE Trans Intell Transp Syst 2015;17(4):1029–38.
[15] Zhang D, Jiang J, Zhang W, et al. Optimal power management in DC microgrids with applications to dual-source trolleybus systems. IEEE Trans Intell Transp Syst 2017;19(4):1188–97.
[16] Bartłomiejczyk M, Jarzebowicz L, Hrbáč R. Application of traction supply system for charging electric cars. Energies 2022;15(4):1448.
[17] Salih M, Baumeister D, Wazifehdust M, Steinbusch P, Zdrallek M, Deskovic P, et al. Impact assessment of integrating novel battery-trolleybuses, PV units and EV charging stations in a DC trolleybus network. In: In 2nd e-mobility power system integration symposium. MOSI Symposium; 2018, p. 1–6.
[18] Paternost RF, Mandrioli R, Barbone R, Cirimele V, Loncarski J, Ricco M. Impact of a stationary energy storage system in a DC trolleybus network. In: 2022 IEEE transportation electrification conference & expo. IEEE; 2022, p. 1211–6.
[19] Diab I, Chandra Mouli GR, Bauer P. Toward a better estimation of the charging corridor length of in-motion-charging trolleybuses. In: 2022 IEEE Transportation Electrification Conference & Expo. 2022, p. 557–62. http://dx.doi.org/10.1109/ITEC53557.2022.9814021.
[20] Diab I, Eggermont R, Mouli GRC, Bauer P. An adaptive battery charging method for the electrification of diesel or CNG buses as in-motion-charging trolleybuses. IEEE Trans Transp Electrif 2023;1. http://dx.doi.org/10.1109/TTE.2023.3243022.
[21] Diab I, Chandra Mouli GR, Bauer P. A review of the key technical and non-technical challenges for sustainable transportation electrification: A case for urban catenary buses. In: 2022 IEEE 20th International Power Electronics and Motion Control Conference (PEMC). 2022, p. 439–48. http://dx.doi.org/10.1109/PEMC51159.2022.9962840.

[22] Wazifehdust M, Baumeister D, Salih M, Steinbusch P, Zdrallek M, von Kalben C, et al. Predictive flexibility calculation for battery-trolleybuses. In: ETG-Kongress 2021 - von komponenten bis zum gesamtsystem fur die energiewende, Vol. 9. 2021, p. 191–6.
[23] Wazifehdust M, Baumeister D, Salih M, Koch M, Steinbusch P, Zdrallek M, Mour S, et al. Potential analysis for the integration of renewables and EV charging stations within a novel LVDC smart-trolleybus grid. In: International conference on electricitiy distribution. 2019, p. 5.
[24] Weisbach M, Spaeth U, Schmuelling B, Troullier C. Flexible EV charging strategy for a DC catenary grid. In: 2020 fifteenth international conference on ecological vehicles and renewable energies. Monte-Carlo, Monaco: IEEE; 2020, p. 1–6. http://dx.doi.org/10.1109/EVER48776.2020.9243038.
[25] Salih M, Koch M, Baumeister D, Wazifehdust M, Steinbusch P, Zdrallek M. Adapted Newton-raphson power flow method for a DC traction network including non-receptive power sources and photovoltaic systems. In: 2019 IEEE PES innovative smart grid technologies europe. Bucharest, Romania: IEEE; 2019, p. 1–5. http://dx.doi.org/10.1109/ISGTEurope.2019.8905722.
[26] Bartłomiejczyk M, Połom M. The impact of the overhead line's powersupply system spatial differentiation on the energy consumption of trolleybustransport: Planning and economic aspects. Transport 2015;32(1):1–12. http://dx.doi.org/10.3846/16484142.2015.1101611.
[27] Bartłomiejczyk M, Połom M. Multiaspect measurement analysis of breaking energy recovery. Energy Convers Manage 2016;127:35–42. http://dx.doi.org/10.1016/j.enconman.2016.08.089.
[28] Bartłomiejczyk M. Smart grid technologies in electric power supply systems of public transport. Transport 2018;33(5):1144–54. http://dx.doi.org/10.3846/transport.2018.6433.
[29] Bartłomiejczyk M. Bilateral power supply of the traction network as a first stage of smart grid technology implementation in electric traction. In: Szeląg A, Karwowski K, Gold H, Żurkowski A, editors. MATEC web of conferences, Vol. 180. 2018, p. 02003. http://dx.doi.org/10.1051/matecconf/201818002003.
[30] Smith K, Galloway S, Burt G. A review of design criteria for low voltage DC distribution stability. In: 2016 51st international universities power engineering conference. Coimbra: IEEE; 2016, p. 1–6. http://dx.doi.org/10.1109/UPEC.2016.8114089.
[31] Smith K, Hunter L, Galloway S, Booth C, Kerr C, Kellett M. Integrated charging of EVs using existing LVDC light rail infrastructure: a case study. In: 2019 IEEE third international conference on DC microgrids. Matsue, Japan: IEEE; 2019, p. 1–7. http://dx.doi.org/10.1109/ICDCM45535.2019.9232726.
[32] Dragicevic T, Guerrero JM, Vasquez JC. A distributed control strategy for coordination of an autonomous LVDC microgrid based on power-line signaling. IEEE Trans Ind Electron 2014;61(7):3313–26. http://dx.doi.org/10.1109/TIE.2013.2282597.
[33] Santos P, Fonte P, Luis R. Improvement of DC microgrid voltage regulation based on bidirectional intelligent charging systems. In: 2018 15th international conference on the european energy market. Lodz: IEEE; 2018, p. 1–6. http://dx.doi.org/10.1109/EEM.2018.8469991.
[34] Zhang T, Zhao R, Ballantyne EE, Stone D. Increasing urban tram system efficiency, with battery storage and electric vehicle charging. Transp Res Part D: Transp Environ 2020;80:102254. http://dx.doi.org/10.1016/j.trd.2020.102254.
[35] Zhang T, Ballantyne EE, Zhao R, Stone DA. Technical and economic feasibility of increasing tram system efficiency with EV batteries. Transp Res Part D: Transp Environ 2021;91:102681. http://dx.doi.org/10.1016/j.trd.2020.102681.
[36] Brand T. Arnhems trolleybusnet onderzoek bovenleidingnet. Liandon (Alliander) & Connection; 2012.
[37] CENELEC. EN 50163 - railway applications - supply voltages of traction systems. Brussels, Belgium; 2004.
[38] Barbone R, Mandrioli R, Ricco M, Paternost RF, Cirimele V, Grandi G. Novel multi-vehicle motion-based model of trolleybus grids towards smarter urban mobility. Electronics 2022;11(6):915.
[39] Brunton L. The trolleybus story. IEE Rev 1992;38(2):57–61.
[40] Vermeer W, Chandra Mouli GR, Bauer P. A multi-objective design approach for PV-battery assisted fast charging stations based on real data. In: 2022 IEEE transportation electrification conference & expo. 2022, p. 114–8. http://dx.doi.org/10.1109/ITEC53557.2022.9814016.
[41] Chandra Mouli GR, Schijffelen J, van den Heuvel M, Kardolus M, Bauer P. A 10 kW solar-powered bidirectional EV charger compatible with chademo and COMBO. IEEE Trans Power Electron 2019;34(2):1082–98. http://dx.doi.org/10.1109/TPEL.2018.2829211.
[42] Sadeghian O, Oshnoei A, Mohammadi-Ivatloo B, Vahidinasab V, Anvari-Moghaddam A. A comprehensive review on electric vehicles smart charging: Solutions, strategies, technologies, and challenges. J Energy Storage 2022;54:105241.
[43] Chymera MZ, Renfrew AC, Barnes M, Holden J. Modeling electrified transit systems. IEEE Trans Veh Technol 2010;59(6):2748–56.
[44] Barbone R, Mandrioli R, Ricco M, Paternost RF, Cirimele V, Grandi G. Novel multi-vehicle motion-based model of trolleybus grids towards smarter urban mobility. Electronics 2022;11(6):915. http://dx.doi.org/10.3390/electronics11060915.
[45] Danner D, de Meer H. Quality of service and fairness for electric vehicle charging as a service. Energy Inform 2021;4:1–20.
[46] Erol-Kantarci M, Sarker JH, Mouftah HT. Quality of service in plug-in electric vehicle charging infrastructure. In: 2012 IEEE International Electric Vehicle Conference. IEEE; 2012, p. 1–5.
[47] ELAAD. ElaadNL Open Datasets for Electric Mobility Research, https://platform.elaad.io/analyses/ElaadNL_opendata.php.
[48] Tomar AS, Veenhuizen B, Buning L, Pyman B. Estimation of the size of the battery for hybrid electric trolley busses using backward quasi-static modelling. In: Multidisciplinary digital publishing institute proceedings, Vol. 2, no. 23. 2018, p. 1499.
[49] Bartłomiejczyk M. Dynamic charging of electric buses. Gdańsk University of Technoligy, Faculty of Electrical and Control Engineering; 2018, https://books.google.cz/books?id=ziX_vQEACAAJ.